EUROPEAN ORGANIZATION FOR NUCLEAR RESEARCH

CERN/EP 79-125
18 October 1979

NEUTRINO AND MUON FLUXES IN THE CERN 400 GeV PROTON BEAM DUMP EXPERIMENTS

H. Wachsmuth
CERN, Geneva, Switzerland

CERN LIBRARIES, GENEVA
CM-P00062309

ABSTRACT

The experimental set-up of the CERN 1979 beam dump experiments is briefly described. Neutrino (ν_μ, $\bar{\nu}_\mu$, ν_e, $\bar{\nu}_e$) spectra from $\pi_{\mu 2}$, $K_{\mu 2}$, K_{e3}, Λ_{e3}, Σ_{e3} decays in the 400 GeV proton beam dump are given based on: (a) pion and kaon production data measured in 400 GeV pBe collisions, adjusted to pCu collisions from 24 GeV pBe and pCu production data and (b) the muon fluxes measured in the shielding 400 m downstream of the dump at three dump (copper) densities (9, 4.5, and 3 g/cm^3). Also given is the neutrino spectrum due to $D\bar{D}$ assumed to be produced like $(1-x)^n e^{-bp_t}$ and to decay into $K^{(*)}\ell\nu$.

HW/mk

1. INTRODUCTION

One reason for the uncertainty in the magnitude of the prompt neutrino fluxes derived from the 1977 CERN beam dump experiments [1-4] was the assumed error of ± 30% in the conventional neutrino fluxes (from π, K, etc. decays). This error reflected the ignorance about production of pions and kaons in 400 GeV proton copper collisions and thick target effects. Since pion and kaon production in a beam dump absorbing all secondaries is not directly measurable, muon fluxes measured downstream of the hadron cascade in the beam dump must be used to derive the conventional neutrino fluxes. Pions and kaons however, have only a small probability to decay before absorption and a large fraction of the muon fluxes will be due to other sources like photo conversion, electromagnetic decays of vector mesons (ρ, ω, ϕ, ψ etc.) or semileptonic decay of higher flavour particles. Muons from these sources - except the last one - are not accompanied by neutrinos. Because of the promptness of these muons (either directly produced or from parents with lifetimes < 10^{-12} s) they can be separated from the π and K decay muons. For the 1979 beam dump experiments muon fluxes were measured from three copper dump targets (massive copper of density ρ = 9 g/cm^3, and disk arrangements of average densities 4.5 and 3 g/cm^3). The prompt muon flux component can now be obtained from the muon flux intensities measured with the three target densities by extrapolation to infinite density; the decay muon fluxes are then obtained by subtraction. The relative contributions from positive and negative pions and kaons must be known in order to determine ν_μ and $\bar{\nu}_\mu$ spectra separately. They are derived from recently measured production data; these data had been taken for the standard target material (beryllium) and geometry ($\lesssim$ 1 absorption length) and hence represent the production in thin target pBe collisions. Production data taken at 24 GeV in several target materials including copper are used to adjust the pBe data to pCu data. The correct energy distribution of the pions and kaons softened by the cascade effect can be found by fitting the calculated muon energy distribution to the muon fluxes measured in several depths in the shielding.

2. EXPERIMENTAL SET-UP

The experimental layout for the 1979 CERN 400 GeV proton beam dump experiments is shown in fig. 1(a). Fig. 1(b) shows details of the construction of the three dumps. The effective dump densities of 4.5 and 3 g/cm^3 were achieved by arranging copper disks of 27 cm diameter and of 2 cm thickness spaced by 2 cm and 4 cm, respectively, over a total length of 2.6 m, enough material to absorb $\sim$ 99% of the primary protons. The effect of the granularity of the dump on the pion flux at any point is < 0.8% difference with respect to a homogeneous dump. The dumps were water cooled. 72% of the experiments were made with the full density dump, 28% with the 3 g/cm^3 dump, and during a short test run (without the neutrino detectors) the 4.5 g/cm^3 dump was used.

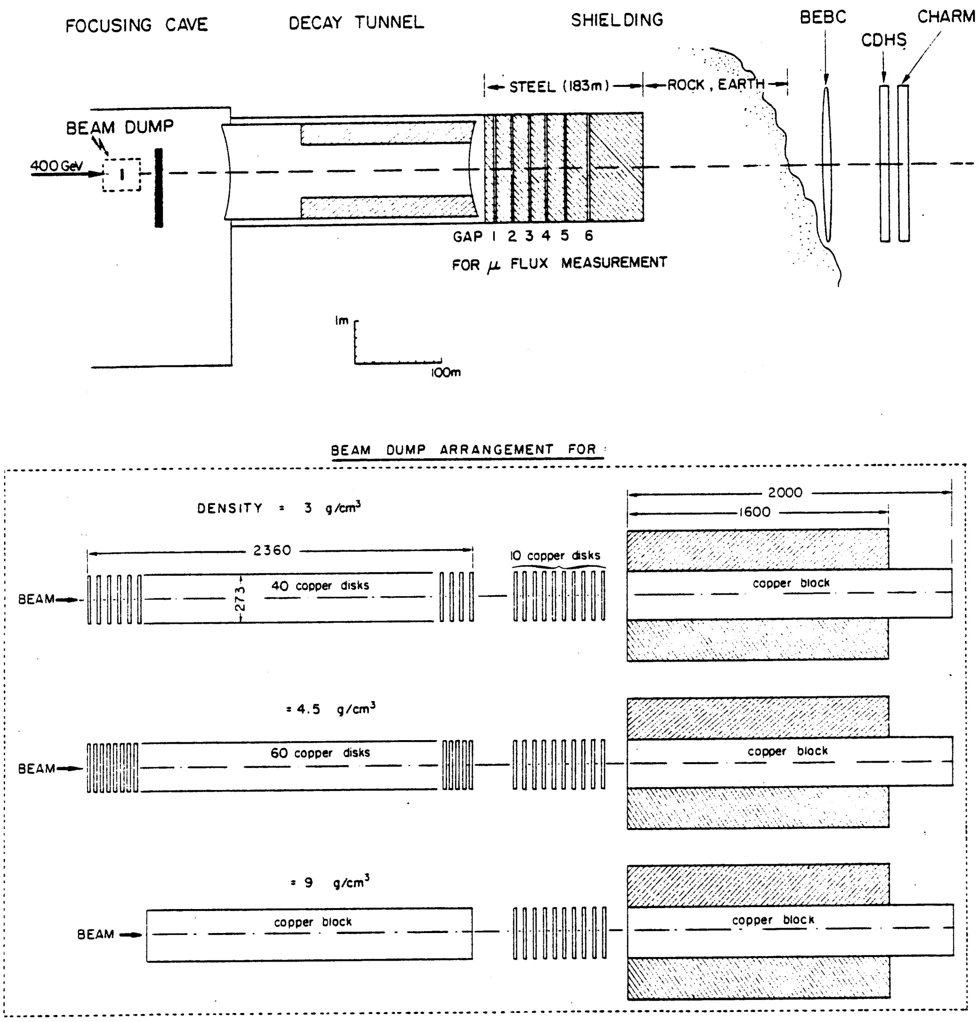

Fig. 1(a) Layout for CERN 1979 beam dump experiments;
(b) details of dump construction.

In order to ensure that neutrino fluxes come mainly from interactions and decays within the dump and not from proton interactions with the vacuum chamber wall upstream of the dump, the signals of eight radiation monitors (ionization chambers) installed along the ejected proton beam line (fig. 2) were recorded continuously. These scraping monitors were calibrated such that a proton beam loss of 1.7×10^{-4} - created by flipping 70 μm thick aluminium foils (beam position detectors) into the beam - induced $\sim$ 2 V or 20% of the full scale signal in the monitors at 10^{13} protons per pulse. It is estimated that such proton interactions would increase the conventional dump flux by 15 to 30%. During the experiments attention was paid that these signals stayed below 50 mV thus keeping scraping contributions negligible.

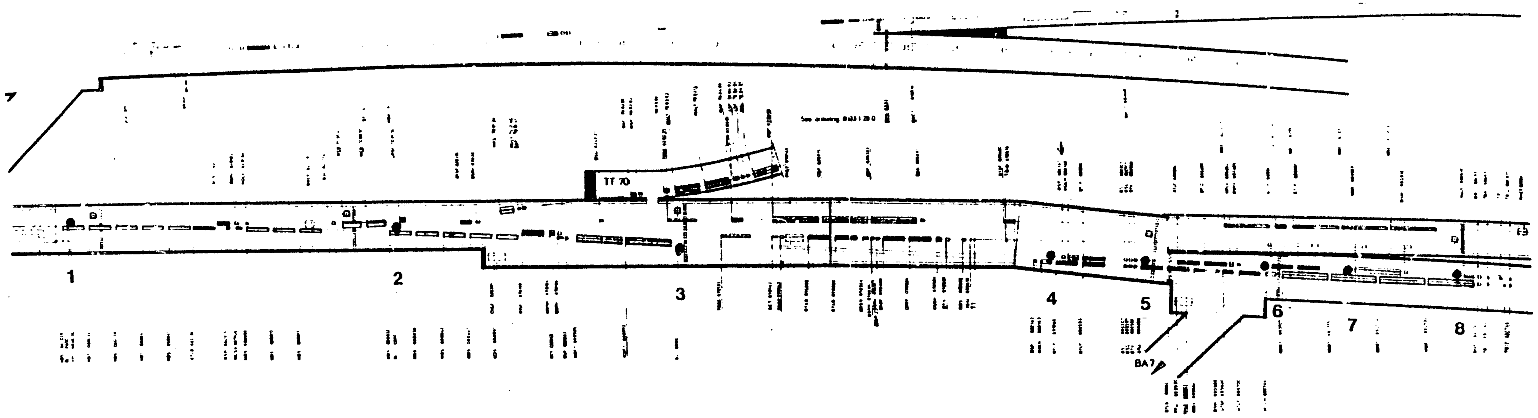

Fig. 2

Scraping monitor (ionization chamber) arrangement:

Number	Distance (m) from dump
1	194
2	149
3	110
4	60
5	48
6	32
7	20
8	5

The beam is bent by 25.5 mr between number 1 and 3 and by -5.5 mr between number 7 and 8. Beam position monitors (70 μ thick split aluminium foils) are at 218, 171, 125, 60, 50, 35, 12 and 3 m distance from the dump.

The muon fluxes were measured using a system of solid state detectors, the charge signals of which were recorded pulse-by-pulse by a computerized data acquisition system [5]. Measurements were done in the first four gaps of the shielding (cf. fig. 1) which correspond to minimum muon momenta of 23, 57, 94, and 136 GeV/c (momentum loss in the dump and momentum slit material taken into account). The detectors had been calibrated previously during wideband neutrino beam experiments in terms of muons per charge unit by counting tracks in nuclear emulsions and separating tracks due to muons from those due to delta rays by their different angular distributions. Last adjustments were made on the basis of relative calibrations performed during the beam dump experiment. Table 1 enumerates the detectors used and their sensitivities, which have a calibration uncertainty of ± 6%.

TABLE 1

Number and sensitivities in muons/picoCoulomb of solid state detectors used during the 1979 beam dump experiments

Gap 1	Detector number sensitivity (μ's/pC)	301 100.	347 105.	17 183.	18 105.	19 166.	20 184.	21 106.	310 155.
Gap 2	Detector number sensitivity	13 36.7	359 44.4	39 37.7	89 45.0	44 45.0	61 39.0	62 41.4	63 36.0
Gap 3	Detector number sensitivity	365 19.4	8 19.0	15 21.0					
Gap 4	Detector number sensitivity	397 23.0	370 17.7						

The proton intensity was measured using the first beam current transformer in the ejected proton beam line. The proton beam was fast extracted (23 μs spill time).

3. PION AND KAON PRODUCTION DATA

In order to determine from muon fluxes neutrino and antineutrino spectra separately and over the whole energy range, the relative contributions from positive and negative pions and kaons must be known. These were measured in 400 GeV pBe collisions in a recent particle production experiment [6] at transverse momenta of 0 and 500 MeV/c and longitudinal momenta p_L of 60, 120, 200 and 300 GeV/c with a relative precision of ± 3%. Those data were corrected for the difference of production in Be and Cu by scaling (in $x = p_L/p_0$)

particle production ratios measured in different target materials at 24 GeV/c proton momentum [7] to a proton momentum p_0 of 400 GeV/c (table 2). The resulting fluxes are shown in fig. 3. A further correction has to be applied to account for the softening of the production spectra in forward direction due to thick target effects (sect. 5). Fig. 4 shows the p_t acceptance of pions produced in the dump for neutrinos above 10 GeV observed in BEBC and muons measured in the shielding (> 25 GeV). The angular acceptance of BEBC is 1.8 mr (half angle) or 10 μsr.

TABLE 2

Ratio of particle production in Cu relative to Be measured at 17 mr and 24 GeV/c proton momentum and applied at zero mr and 400 GeV/c.

x = p/24	0.17	0.25	0.42	0.58	0.75
p(400 GeV)	70.	100.	170.	230.	300.
π^+	0.98	0.82	0.77	0.70	0.66
π^-	1.01	0.90	0.80	0.82	0.66
K^+	1.18	1.05	0.86	0.76	0.70
K^-	1.07	0.93	0.78	0.68	0.71

4. MUON FLUX DATA

The three upper curves in fig. 5(a) show the muon fluxes measured in the first four gaps of the shielding for the three dump densities. The data are flux intensities averaged over a circle of 40 cm radius around the beam axis. The radial distributions are flat.

Since the three dumps consist of different amounts of material (fig. 1(b)) the measured muon fluxes must be corrected for the difference in multiple scattering (and energy loss). This has been done by a Monte-Carlo calculation: if the 1/3 (1/2) density dump had consisted of the same amount of material as the full density dump the measured muon fluxes would have been 1.19 ± 0.04 (1.12 ± 0.03) times lower. The flux data in fig. 5(b) are normalised to the full density dump.

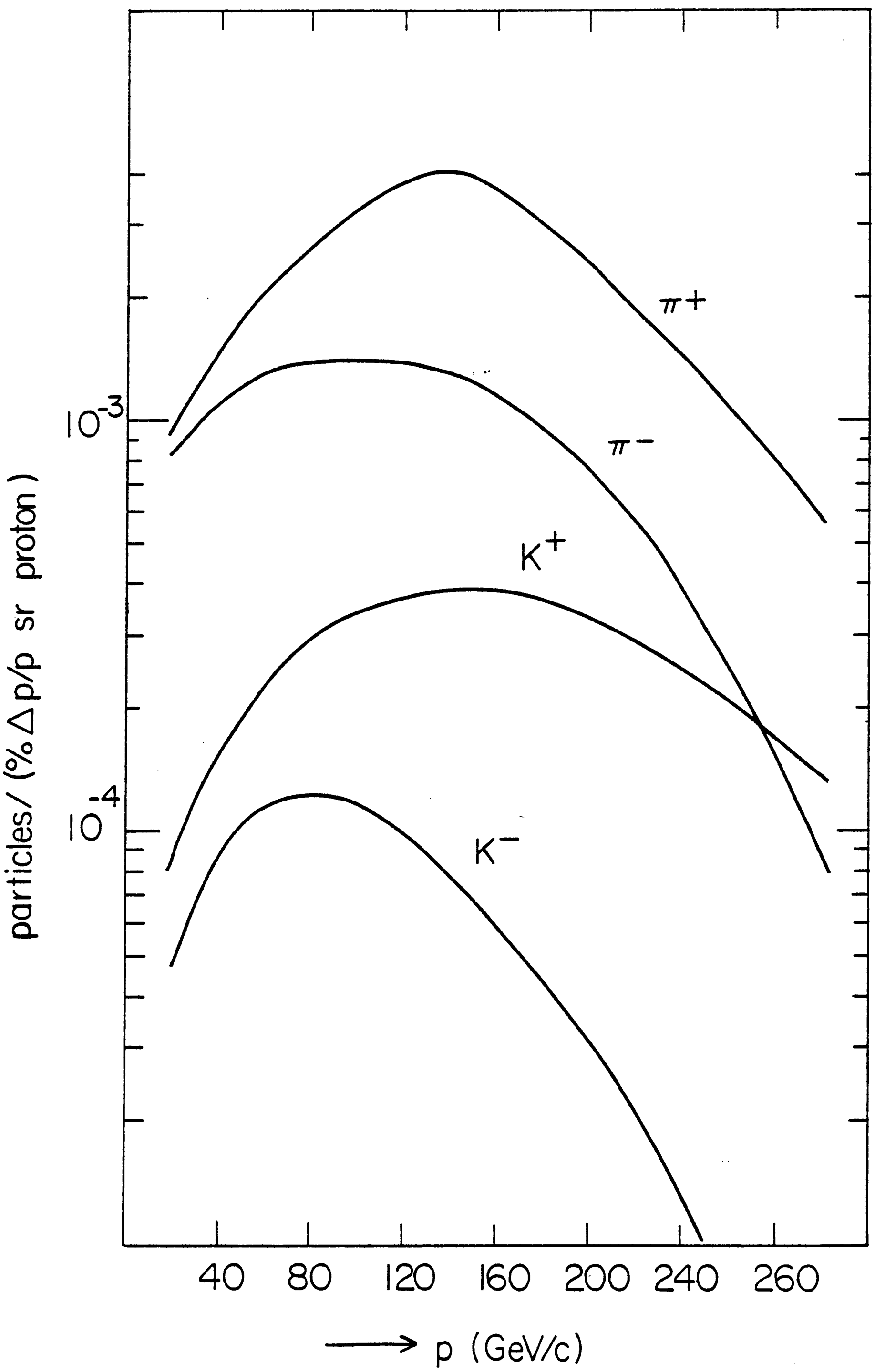

Fig. 3

Particle production in 400 GeV proton copper collisions for $p_t = 0$.

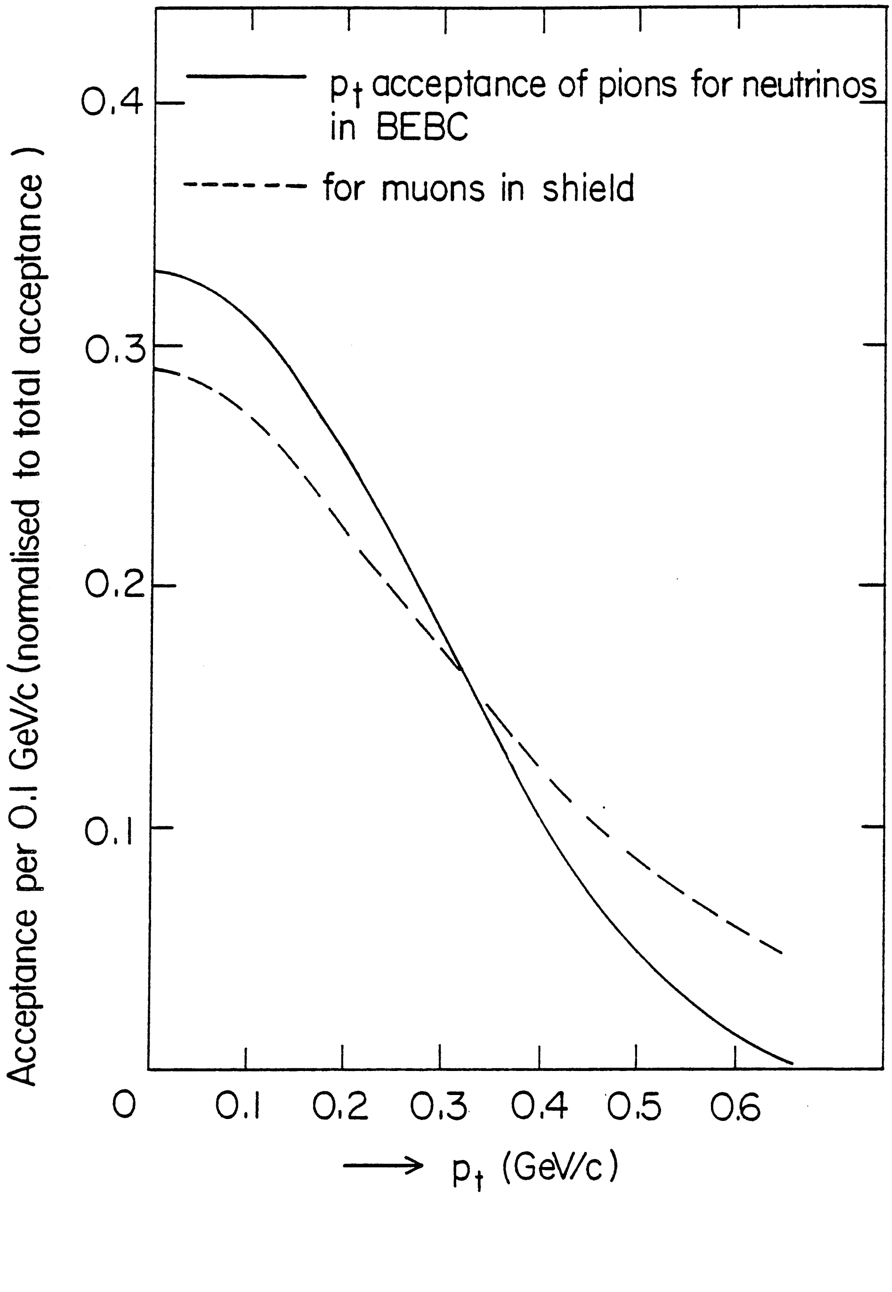

Fig. 4

p_t acceptance of pions for neutrinos in BEBC and muons in shield.

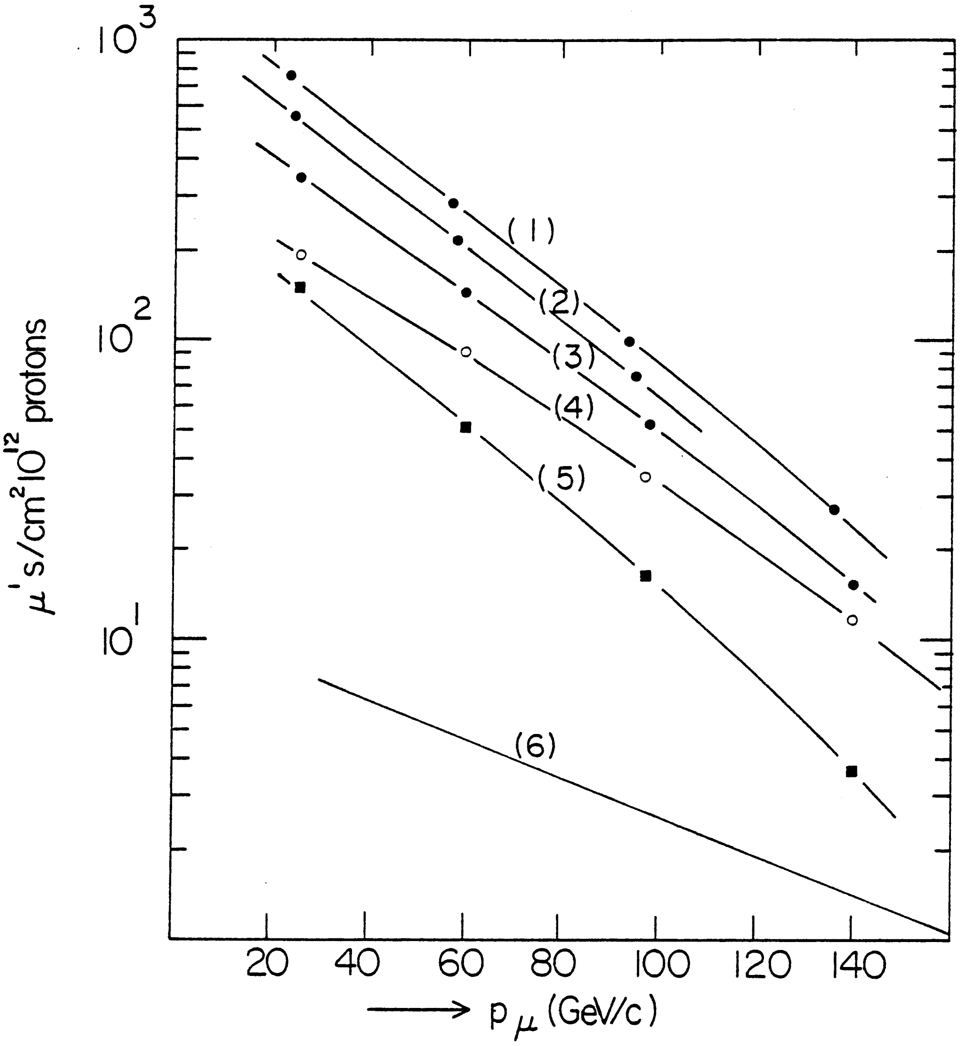

Fig. 5(a)

Muon fluxes above p_t measured with ρ_{dump}/ρ_{Cu} = 1/3 (curve 1), = 1/2 (curve 2), = 1 (curve 3).

Curve 4: prompt muon flux above p_t obtained from fig. 5(b).

Curve 5: decay fluxes (difference between curves 3 and 4).

Curve 6: $10^4(\mu/\pi^+)_{prompt}$ = 1.5 exp (-0.015 p_μ).

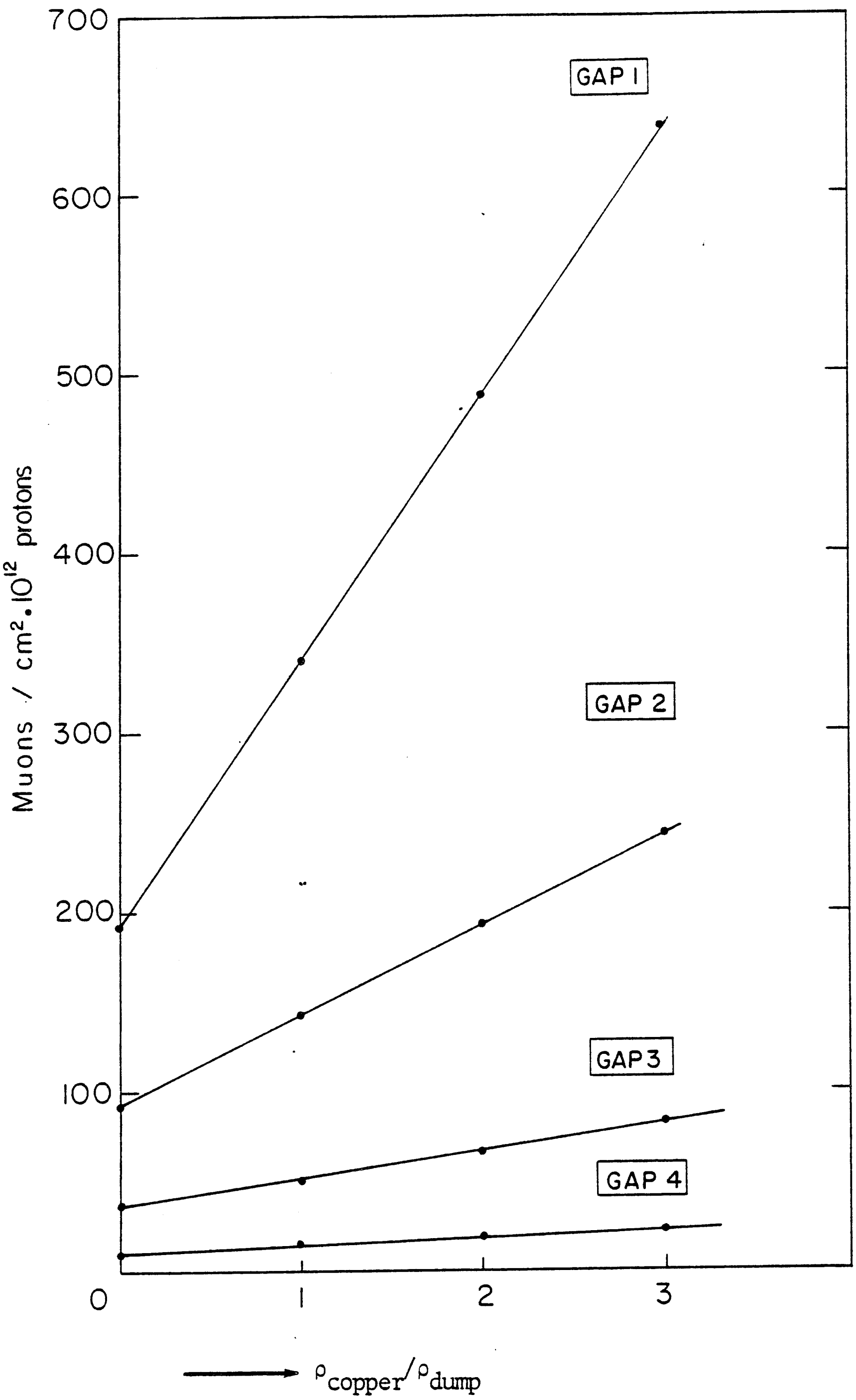

Fig. 5(b)

Muon fluxes (corrected for different amounts of dump material, see text) as functions of $1/\rho$.

From fitting straight lines through the muon flux data as functions of the reciprocal density (fig. 5(b)) the prompt muon fluxes (μ^+_{pr} + μ^-_{pr}) are obtained as the intercepts at $1/\rho = 0$. These and the decay muon fluxes (μ^+_d + μ^-_d) are also drawn in fig. 5(a). The relative uncertainties from fitting and subtracting are about ± 4% on all points.

Some fraction of the mesons will survive the low density dump and decay downstream of it and fake prompt muons. Since the number of absorption lengths is different in the two lower density dumps (7.7 in the case of density 1/2 and 5.5 in the 1/3 density dump) this would lead to a non-linear increase of the muon flux with ρ_{Cu}/ρ_{dump}. From the observed linearity (better than 2%) it can be concluded that such a correction is contained within the ± 4% uncertainty. It should be noted that muon fluxes are measured out to a maximum angle of 1 mr with respect to the dump.

From the measured (400 GeV pBe) and extrapolated (from 24 GeV pBe and pCu) π and K production data, the relative contribution of positive and negative muons in the decay muon flux can be calculated with an accuracy of ± 5% (2-3% from direct particle ratios, 4-5% by applying 24 GeV/c Cu/Be ratios at 400 GeV/c proton momentum). Including the uncertainty in the absolute calibration (± 6%) and due to multiple scattering (± 6%), the positive and negative decay muon fluxes are thus determined with about ± 10% precision.

Also shown in fig. 5(a), (curve (6)) is the result of an attempt to fit the global $\mu^+_{pr}/\pi^+ (= \mu^-_{pr}/\pi^+)$ ratio necessary to reproduce the prompt muon fluxes measured in the shielding (curve (4)).

5. "CONVENTIONAL" NEUTRINO FLUXES

In order to determine the conventional ν_μ (and ν_e) fluxes, the π and K fluxes of fig. 3 have to be corrected for thick target effects. This is done by fitting the calculated to the measured decay muon fluxes varying the absolute number and momentum distribution of the pions. The calculation assumes a simple model where all protons interact in the beginning of the dump and the whole nuclear cascade in the dump is replaced by a decay path of one absorption length (18 cm for pions, 21 cm for kaons [8]). The muon fluxes thus predicted are lower at low energies and higher at high energies than the measured muon fluxes (table 3). The measured decay fluxes, curve (5) of fig. 5(a) are separated into positives and negatives according to the π^+, π^-, K^+ and K^- fluxes of fig. 3.

TABLE 3

Muons fluxes from $\pi_{\mu 2}$ and $K_{\mu 2}$ decays in the dump predicted, measured and fitted, averaged over a circle of 0.375 m radius around the beam axis.

	Positive (μ^+)				Negative (μ^-)				
p_{min}	25	60	97	140	25	60	97	140	GeV
Measured (dump)	100.	36.9	12.5	2.92	47.	13.6	3.80	0.78	Muons per
Predicted (thin target)	66.7	32.4	13.5	4.5	31.5	11.9	4.08	1.21	cm^2 and
Fitted	99.3	37.8	12.1	2.95	46.6	14.0	3.66	0.79	10^{12} protons

The adjustment of the pion(and kaon) spectra to fit this muon flux distribution can be done either by multiplying them by an arbitrary polynomial in p or by superimposing π spectra from four proton generations (400, 268, 180, and 120 GeV protons according to $E_i = E_0\ (1 - k)^i$ and inelasticity $k = 1/3$). The fitting results in a depletion of high energy (by $\sim$ 40% at 200 GeV) and increase of low energy pions ($\sim$ 80% at 40 GeV). The various fits give within 3% the same neutrino spectra per muon flux, and hence the overall absolute error on the conventional neutrino spectra is believed to be essentially the error with which the μ^+ and μ^- fluxes from π and K decays can be determined separately ($\pm$ 10%). Below 10 GeV the error is larger since the muon fluxes are measured above 23 GeV and the π and K production measurements were not done below 60 GeV.

Electron-neutrino fluxes are calculated from K_{e3} decays assuming equal K^+ and K^0 (K^- and $\bar{K}^0$) production per pCu collision. Thermodynamic model predictions [9] have been used for Λ and Σ^- production (accounting for about $\frac{1}{2}$ of the $\bar{\nu}_e$ flux). The resulting spectra are shown in fig. 6 and table 4.

Assuming $10^{38} \cdot \sigma/E = 0.62 \pm 0.03$ for charged current neutrino and 0.30 ± 0.02 for antineutrino interactions [10] event rates from conventional neutrinos can be predicted. They are given in table 5 for a distance of 820 m downstream of the dump (position of BEBC) per ton and 10^{18} protons.

TABLE 4

Conventional neutrino fluxes from CERN 400 GeV beam dump per ($m^2 \cdot GeV \cdot 10^{10}$ protons) averaged over 1.8 m detector radius at 820 m distance.

E_ν	ν_μ From $\pi_{\mu 2} K_{\mu 2}$	ν_μ From $K_{\mu 3}$	ν_μ Total	ν_e Total $(3 \times K^+_{e3})$	$\bar{\nu}_\mu$ From $\pi_{\mu 2}, K_{\mu 2}$	$\bar{\nu}_\mu$ From K, Λ, Σ	$\bar{\nu}_\mu$ Total	$\bar{\nu}_e$ From K_{e3}	$\bar{\nu}_e$ From Λ_{e3}	$\bar{\nu}_e$ From Σ^-_{e3}	$\bar{\nu}_e$ Total
(GeV)											
0-5	926.	7.21	933.	10.6	583.	5.1	588.	7.35	0.2	0.08	7.63
5-10 a)	418.	11.6	430.	17.1	288.	7.0	295.	10.	0.8	0.18	11.0
10-15 a)	205.	7.6	213.	11.1	133.	4.3	137.	5.7	1.2	0.36	7.16
15-20	147.	6.14	153.	9.03	84.7	3.25	88.	4.1	1.3	0.47	5.87
20-25	90.7	4.35	95.	6.39	47.	2.3	49.3	2.69	1.2	0.56	4.45
25-30	74.1	3.12	77.2	4.59	33.9	1.7	35.6	1.81	1.05	0.58	3.44
30-40	44.7	2.18	46.9	3.21	18.7	1.15	19.9	1.15	0.77	0.52	2.44
40-50	27.5	1.30	28.8	1.91	10.5	0.67	11.2	0.60	0.47	0.39	1.46
50-60	17.1	0.83	17.9	1.22	6.05	0.40	6.45	0.32	0.22	0.32	0.86
60-70	11.0	0.49	11.5	0.73	3.57	0.21	3.78	0.163	0.085	0.19	0.44
70-80	7.0	0.33	7.33	0.48	2.03	0.114	2.14	0.0951	0.026	0.105	0.23
80-90	4.90	0.21	5.11	0.31	1.25	0.058	1.31	0.0525	0.0051	0.050	0.108
90-100	3.52	0.14	3.66	0.20	0.774	0.030	0.80	0.0300		0.018	0.032
100-120	2.13	0.064	2.19	0.094	0.39		0.40	0.0115		0.003	0.0135
120-140	1.14	0.026	1.17	0.038	0.16			0.0048			0.0048
140-160	0.57	0.010	0.58	0.015	0.063						
160-180	0.27	0.003	0.27	0.005	0.024						
180-200	0.13			0.0017	0.0086						
200-220	0.060			0.0005	0.0030						
220-240	0.023				0.0075						
240-260	0.0069				0.00014						
260-280	0.0019				0.00002						

a) Only by extrapolation.

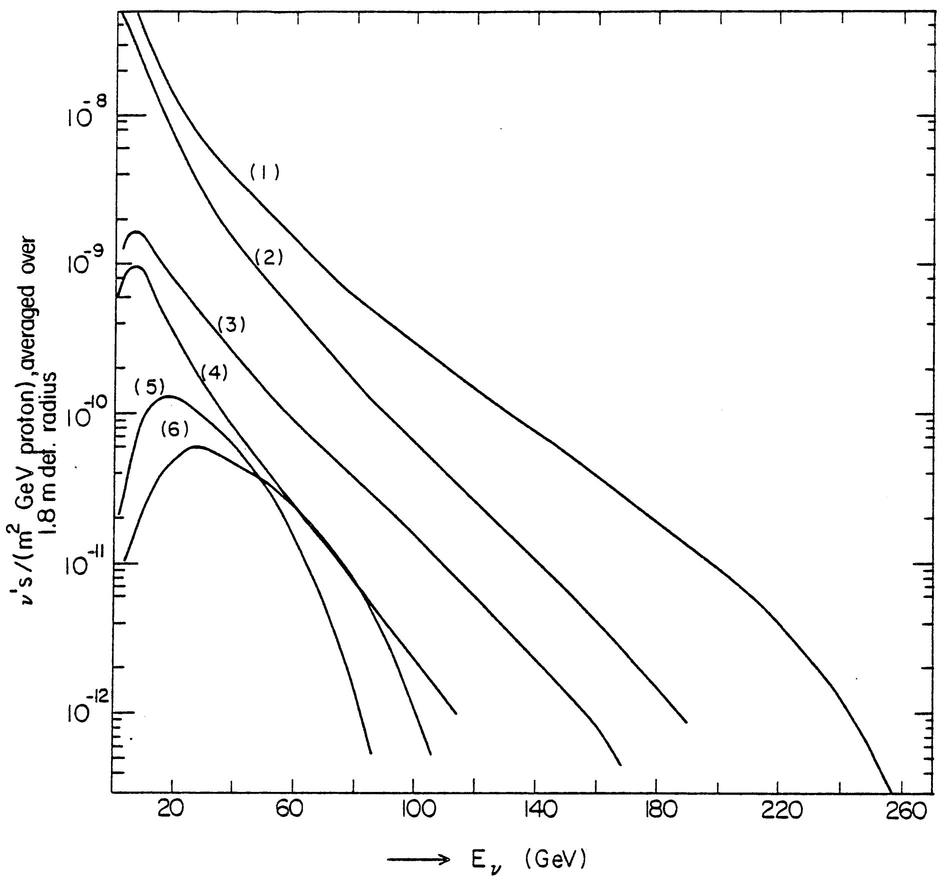

Fig. 6

Conventional neutrino spectra:

(1) ν_μ from $(\pi + K)^+_{\mu 2}$

(2) $\bar{\nu}_\mu$ from $(\pi + K)^-_{\mu 2}$

(3) ν_e from $(K^0, K^+)_{e3}$

(4) $\bar{\nu}_e$ from $(\bar{K}^0, K^-)_{e3}$

(5) $\bar{\nu}_e$ from Λ_{e3}

(6) $\bar{\nu}_e$ from Σ^-_{e3}

TABLE 5

Predicted charged current neutrino event rates (± 11%) from conventional sources (π, K, Λ, Σ decays) produced in the 400 GeV proton beam dump (per ton and 10^{18} protons).

E_{min} (GeV)	ν_μ	ν_e	ν_e/ν_μ	$\bar{\nu}_\mu$	$\bar{\nu}_e$	$\bar{\nu}_e/\bar{\nu}_\mu$	$\bar{\nu}_\mu/\nu_\mu$
10	4.47	0.267	0.060	0.901	0.084	0.093	0.202 ± 0.013
20	3.47	0.212	0.060	0.607	0.067	0.11	0.174 ± 0.011
50	1.57	0.088	0.056	0.201	0.0204	0.10	0.128 ± 0.008
100	0.427	0.015	0.035	0.0295	0.0008	0.027	0.069 ± 0.004

It follows from the discussion about the errors in the flux determination (± 10%) that the uncertainty in these rate predictions including the cross section error should be ± 11%. The error in the predicted ratio of $\bar{\nu}_\mu$ to ν_μ events comes from the $(\pi, K)^-/(\pi, K)^+$ ratios measured in pBe collisions (± (2-3)%) and their extrapolation to pCu collisions (table 2) and the $\bar{\nu}/\nu$ cross section ratio 0.48 ± 0.02 [10] and might be less than the ± 6.5% quoted in table 5. 67% of the conventional e^- events are due to K^0 decays and 80% of the e^+ events are due to $\bar{K}^0$, Λ and Σ^- decays. Hence the errors on the predicted ratios of ν_e/ν_μ and $\bar{\nu}_e/\bar{\nu}_\mu$ events depend largely on the uncertainty in the precision of the relative rate of production of these particles (∿ 10%?).

6. "PROMPT" NEUTRINO FLUXES

Neutrino flux in excess over the conventional one is mostly interpreted in terms of production and semi-leptonic decay of charmed particles [11], [1-4]. As examples, neutrino spectra (Monte-Carlo calculations) due to such sources are given in fig. 7. The model for D production assumed is $E\, d^3\sigma/dp^3 \sim (1-x)^n e^{-bp_t}$ and the spectra in fig. 7 are for n = 3 and 4 and b = 2, and for decays(*) $D \to K\ell\nu$ and $K^*\ell\nu$ with 10% branching ratio each. They are arbitrarily normalized to produce one μ^- (or e^-) event per ton and 10^{18} protons above 10 GeV at the position of BEBC. This would require production cross sections for $\sigma(pp \to D\bar{D} + \text{anything})$ as given in table 6 and would contribute ∿ 20% to the ratio $(\mu/\pi^+)_{prompt}$ (curve 6 of fig. 5(a)).

(*) Using the decay distribution dN/dp^* for $K_{\ell 3}$ scaled by the ratios of p^*_{max}.

The dependence of the cross section on n and b is discussed in ref. [4]. Details of such calculations in analytic form and also for other models can be found in ref. [12]. Secondary, tertiary, etc. protons would also contribute

TABLE 6

D production cross sections per prompt charged current neutrino event above 10 GeV per ton and 10^{18} protons at BEBC position for various hypotheses, if only primary protons contribute and D's do not re-interact in the nucleus (mass number A).

Curve in fig. 7	n	Decay (BR = 10%)	10^3 D's/p	$\sigma \sim \sigma_{pA}^{abs}$ ($= 38.5 \cdot A^{0.72}$) μb	$\sigma \sim A^1$ (μb/nucleon)	$\langle E_{ev} \rangle$ (GeV)
1	3	$Ke\nu$	1.1	43	13.4	91
2	3	$K^*e\nu$	1.4	53	16	76
3	4	$Ke\nu$	1.7	66	21	80
4	4	$K^*e\nu$	2.1	81	25	67

to such D production. A rough estimate of this effect can be made by superimposing D spectra from several proton generations (cf p. 12), weighting their cross sections by $\sqrt{s}$ and normalising the result as before (to one event in BEBC). As a consequence, a ∿ 35% smaller cross section for D production by the primary proton is obtained, and the neutrino energy distributions (fig. 7) are modified (softened) as given in table 7. The angular distribution of protons is neglected; its effect is absorbed in the uncertainty of the parameter b.

TABLE 7

Approximate softening of $\nu_\ell(D_{\ell 3})$ spectra due to proton cascading.

E_ν (GeV)	15	30	50	70	90	110	> 120
Spectrum from four generations / Spectrum from first generation	1.67	1.35	1.11	0.91	0.86	0.82	0.73

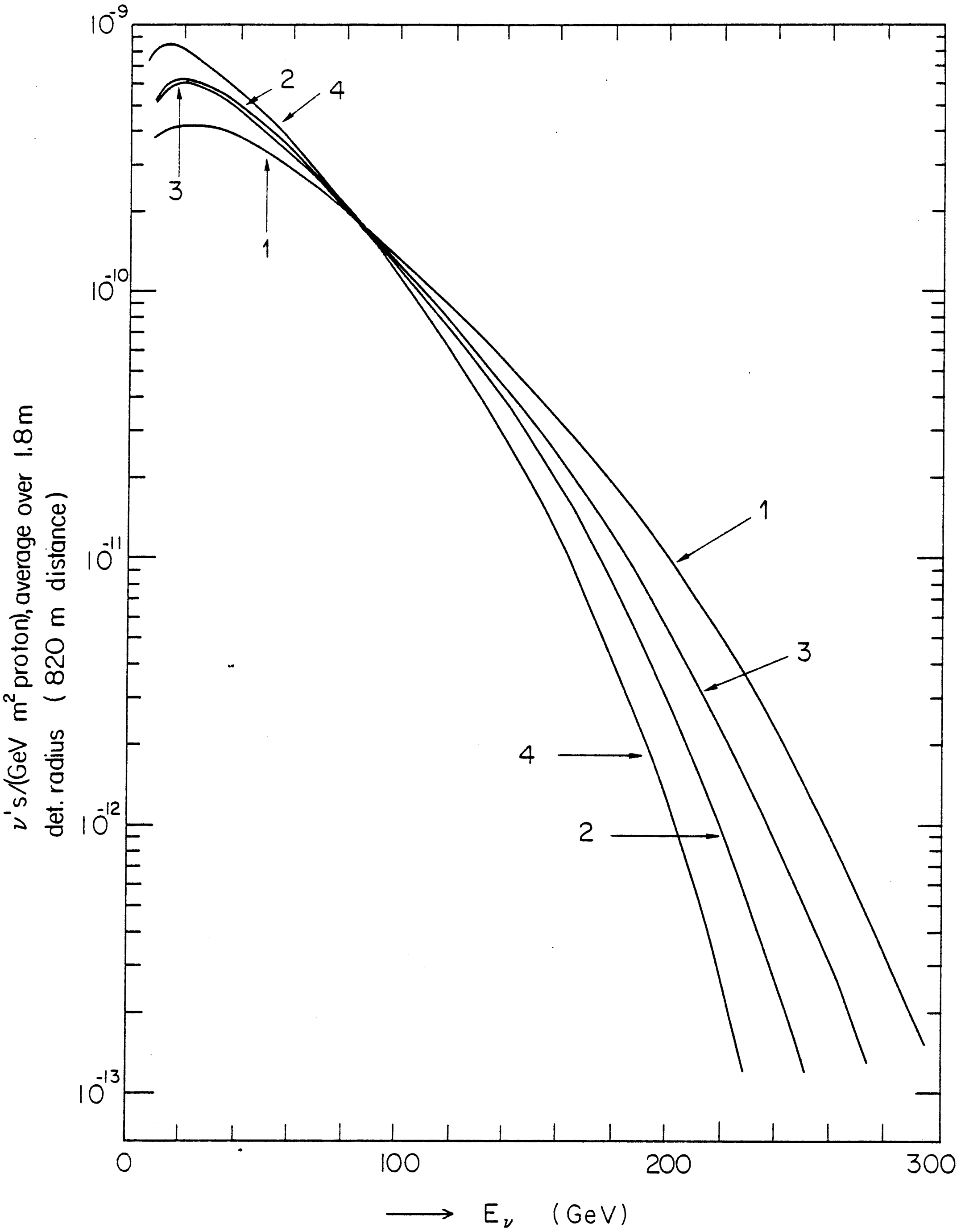

Fig. 7

ν_e (= ν_μ) spectra due to $D_{\ell 3}$ decay (see text) arbitrarily normalized to produce one charged current event per ton and 10^{18} protons 820 m downstream of the beam dump. The numbers on the curves are explained in table 6.

Prompt neutrino flux could also be due to associated production of charmed mesons and baryons like pCu → $\Lambda_c \bar{D}$ + ..., and if the baryon is produed more diffractively than the meson, relatively more neutrinos would be accepted leading to smaller production cross sections and possibly to a ratio of prompt $\nu/\bar{\nu} > 1$. If in addition the Q value of the baryon decay is different from the meson decay, neutrinos and antineutrinos could have different energy spectra.

The possibility that the parent particles re-interact inside the production nucleus is another source of uncertainty in deriving production cross sections from the prompt neutrino flux. Finally, prompt neutrinos could come from sources other than charmed particles.

CONCLUSION

For the 1979 CERN beam dump experiments muon fluxes were measured from dumps of three different densities allowing a determination of the "conventional" neutrino event background (4.5 μ^- events in BEBC per ton and 10^{18} protons) with ± 11% precision. The possibility that events in the neutrino detectors are due to proton interactions upstream of the dump ("scraping") - thus appearing as prompt - could be excluded experimentally using ionization chambers along the beam pipe. Cross sections for the production of sources (e.g. charmed particles) leading to prompt neutrinos will have large uncertainties due to the multitude of parameters affecting intensity and energy distribution of such neutrinos observed ∿ 1000 m downstream of the dump.

Acknowledgements

The author gratefully acknowledges the excellent collaboration with W. Middelkoop, P. Sievers and R. Bellone of the SPS target group in designing and operating the beam dumps, with V. Hatton, L. Evans and their colleagues of the SPS main control room who run a non-scraping proton beam, with G. Cavallari, H. Heijne and P. Jarron in measuring the muon fluxes, with H.J. Klein in analysing the muon flux data, and numerous enjoyable discussions with Ch. Peyrou and many colleagues from all beam dump collaborations.

REFERENCES

[1] P.C. Bosetti et al., Phys. Lett. 74B (1978) 143.

[2] T. Hansl et al., Phys. Lett. 74B (1978) 139.

[3] P. Alibran et al., Phys. Lett. 74B (1978) 134.

[4] H. Wachsmuth, Proc. Topical Conf. on Neutrino Physics, Oxford, 2-7 July 1978 and CERN/EP/PHYS 78-29.

[5] G. Cavallari et al., Proc. Nuclear Science Symposium, San Francisco, 1977.

[6] H. Atherton et al., in preparation.

[7] Th. Eichten et al., Nucl. Phys. B44 (1972) 333.

[8] W. Busza et al., Phys. Rev. Lett. 34 (1975) 836;
S.P. Denisov et al., Nucl. Phys. B61 (1973) 62.

[9] R. Hagedorn and J. Ranft, Nucl. Phys. B48 (1972) 157 and Computer Program SPUKJ, CERN Computer Library.

[10] J.G.H. de Groot et al., Zeitschr. f. Physik. C1 (1979) 143.

[11] B. Pontecorvo, Zh. Eksp. Teor. Fiz. 60 (1975) 452.

[12] K.W.J. Barnham and N.S. Graigie, Nucl. Phys. B154 (1979) 463.